Supporting Information for

Au-based Bimetallic Nanoparticles for the Intramolecular Aminoalkene Hydroamination

Sanjay K. Singh,[a,b] Munendra Yadav,[a] Silke Behrens,*[c] and Peter W. Roesky*[a]

[a] *Institute of Inorganic Chemistry, Karlsruhe Institute of Technology (KIT) Engesserstr. 15, 76131 Karlsruhe,Germany. Fax: ++721 60844854; E-mail: roesky@kit.edu*

[b] *Discipline of Chemistry, School of Basic Science, Indian Institute of Technology (IIT) Indore, IET-DAVV Campus, Khandwa road, Indore 452017, Madhya Pradesh, India; E-mail: sksingh@iiti.ac.in*

[c] *Institut für Katalyseforschung und –technologie (IKFT), Karlsruher Institut für Technolgie (KIT), Hermann-von-Helmholtz-Platz 1, 76344 Eggenstein-Leopoldshafen,; E-mail: silke.behrens@kit.edu*

General: All metal salts were obtained from Aldrich. NMR spectra were recorded on a Bruker Avance 300 spectrometer. Chemical shifts are referenced to internal solvent resonances and are reported relative to tetramethylsilane. GC-MS spectra of selected compounds were recorded by using Double Focusing Sector Mass Spectrometer (DFS). GC was measured on a Trace GC Ultra from Thermo Fisher Scientific using a J&W Scientific column (DB-17ms: 50% dimethyl/ 50% diphenyl polysiloxan) over temperature range of von 40 to 250 °C (10 °C / min). Helium, 0,8 ml/min, was used as flow gas. Electron microscopy (TEM, STEM-HAADF, HRTEM) experiments and elemental analysis (EDX) were performed with a FEI Tecnai F20 ST TEM (operating voltage 200 kV) equipped with a field emission gun and EDAX EDS X-ray spectrometer [Si(Li) detecting unit, super ultra thin window, active area 30 mm^2, resolution 135 eV (at 5.9 keV)]. For TEM analysis, a few droplets of the nanoparticle suspension were deposited onto amorphous carbon-coated 400 mesh copper grids (for AuPt, AuPd and AuNi nanoparticles) and nickel grids (for AuCu nanoparticles) and eventually air dried. Particle sizes and size distributions were statistically evaluated from TEM observations based on typically 100 particles. Powder X-ray diffraction (XRD) studies were performed on the dried particles with a PANalytical X'Pert Pro X-ray diffractometer using Cu Kα radiation. The mean size of the individual nanoparticles d was calculated based on (111), (200), and (220) reflections of the face centred cubic phase of monometallic Au and bimetallic (AuCu, AuPt, AuPd, AuNi) nanopartiles using Scherer equation,

$$d = \frac{0.9\lambda}{\beta \cos\theta}$$

where 0.9 is a shape factor, β the full width at half maximum of the diffraction peak and θ the peak position. LaB_6 (NIST) was measured in order to account for instrumental broadening. Alkeneamine substrate, 2,2-diphenylpent-4-en-1-amine, was prepared using modified literature procedures[1] from commercially available starting materials.

Intramolecular hydroamination of alkeneamines:

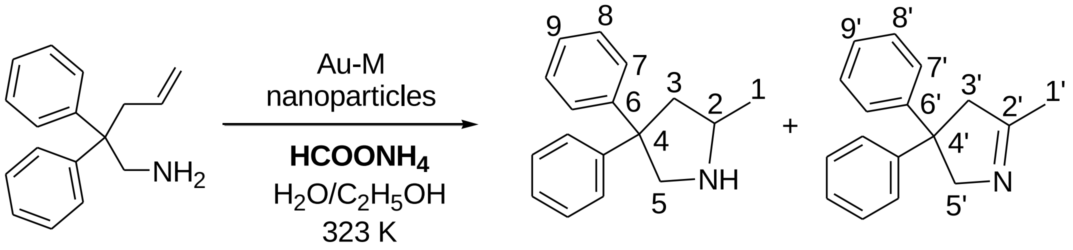

1 **2a** **2b**

2-Methyl-4,4-diphenylpyrrolidine (2a)[1]

^{1}H NMR (300 MHz, $CDCl_3$): δ (ppm) = 7.38-7.13 (m, 10H, Ph), 3.88 (d, 1H, 12Hz, H_5), 3.69 (d, 1H, *J* = 12 Hz, H_5), 3.60 (m, 1H, H_2), 2.76 (dd, 1H, *J* = 12 Hz, H_3), 2.38 (dd, 1H, *J* = 12 Hz, H_3), 1.49 (d, 3H, H_1). **^{13}C{^{1}H} NMR** (75 MHz, $CDCl_3$): *δ* (ppm) = 146.00 (C_6), 145.24 (C_6), 127.46 (C_8), 127.39 (C_8), 125.98 (C_7), 125.92 (C_7), 125.24 (C_9), 55.88 (C_5), 55.71 (C_2), 52.42 (C_3), 45.66 (C_4), 20.24 (C_1).

5-Methyl-3,3-diphenyl-3,4-dihydro-2H-pyrrole (2b)

^{1}H NMR (300 MHz, $CDCl_3$): δ (ppm) = 7.38-7.13 (m, 10H, Ph), 4.48 (s, 2H, $H_{5'}$), 3.24 (s, 2H, $H_{3'}$), 2.12 (s, 3H, $H_{1'}$). **^{13}C{^{1}H} NMR** (75 MHz, $CDCl_3$): *δ* (ppm) = 174.50 ($C_{2'}$), 147.88 ($C_{6'}$), 128.42 ($C_{8'}$), 126.78 ($C_{7'}$), 126.23 ($C_{9'}$), 61.41 ($C_{5'}$), 48.55 ($C_{3'}$), 41.14 ($C_{4'}$), 20.25 ($C_{1'}$).

Catalytic intramolecular hydroamination reaction of 2,2-diphenylpent-4-en-1-amine (1) with $DCOONH_4$ in the presence of AuPt nanoparticle catalyst:

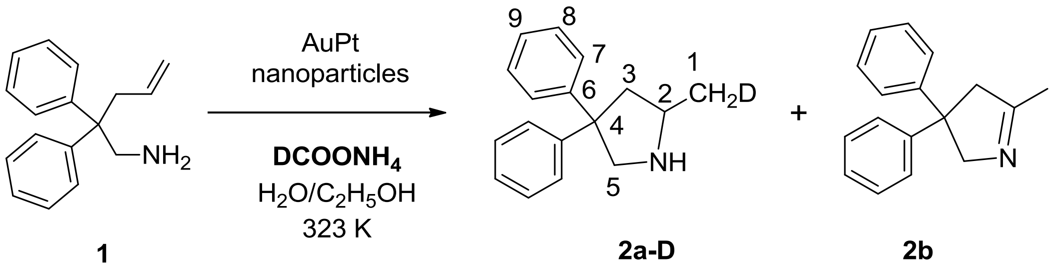

2-Methyl-4,4-diphenylpyrrolidine (2a-D)

^{1}**H NMR** (300 MHz, $CDCl_3$): δ (ppm) = 7.39-7.14 (m, 10H, Ph), 3.81 (d, 1H, 12Hz, H_5), 3.71 (d, 1H, 12 Hz, H_5), 3.62 (m, 1H, H_2), 2.76 (dd, 1H, 12 Hz, H_3), 2.42 (dd, 1H, J = 12 Hz, H_3), 1.52 (t, 2H, H_1). ^{2}**H NMR** (300 MHz, $CDCl_3$): δ (ppm) = 1.30. ^{13}**C{^{1}H} NMR** (75 MHz, $CDCl_3$): δ (ppm) = 146.26 (C_6), 145.52 (C_6), 127.27 (C_8), 127.21 (C_8), 125.86 (C_7), 125.80 (C_7), 124.99 (C_9), 56.24 (C_5), 55.87 (C_2), 52.07 (C_3), 45.71 (C_4), 20.29 (t, C_1, J = 18.7 Hz).

$^{13}C\{^{1}H\}$ NMR spectrum of 2-Methyl-4,4-diphenylpyrrolidine (**2a-D**) showing the triplet of the methyl group at 20.29 ppm.

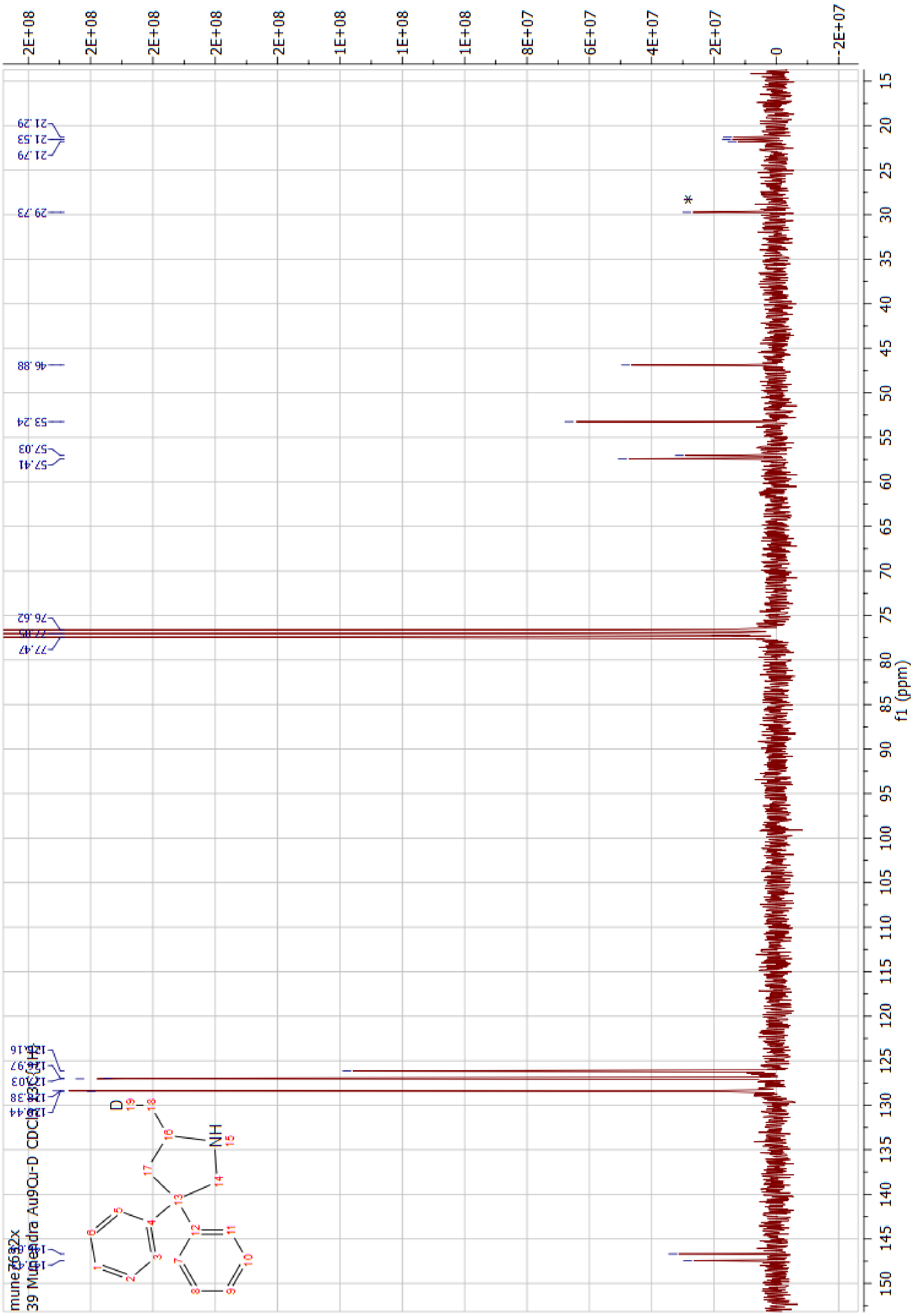

Comparative GC-MS results: The catalytic intramolecular hydroamination of alkeneamines (2,2-diphenylpent-4-en-1-amine) for the formation of hydroaminated pyrrolidine product (**2a**) and the cyclic imine product (**2b**), in the presence of Au-M (M = Cu and Pt) nanoparticles catalysts.

Scan rate: 2.57e-004 hz

Catalyst	**2-methyl-4,4-diphenylpyrrolidine (2a)**		**5-methyl-3,3-diphenyl-3,4-dihydro-2H-pyrrole (2b)**	
	NMR	**GC**	**NMR**	**GC**
AuCu	**96.62 %**	**96.63 %**	**3.38 %**	**3.37 %**
AuPt	**68.74 %**	**61.40 %**	**31.26 %**	**38.60 %**

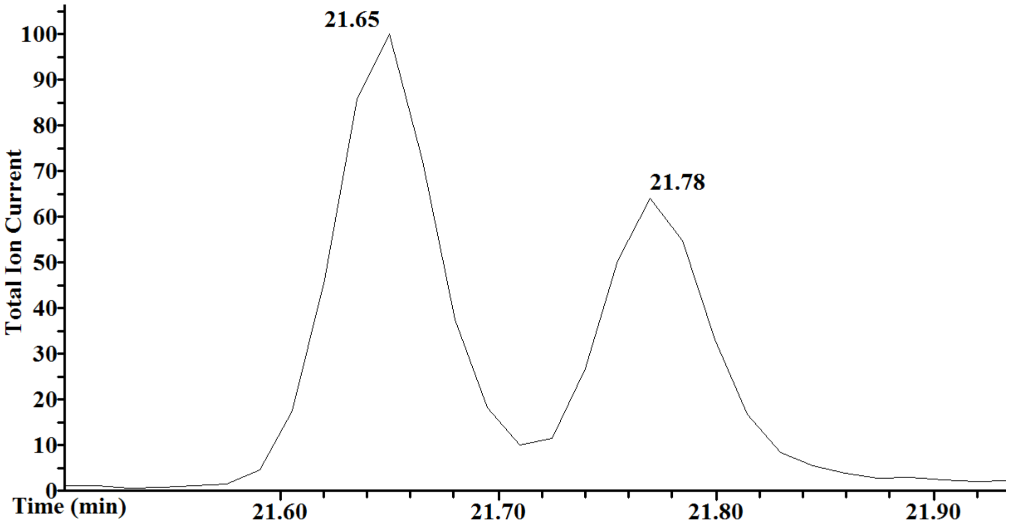

Catalyst = AuPt nanoparticles

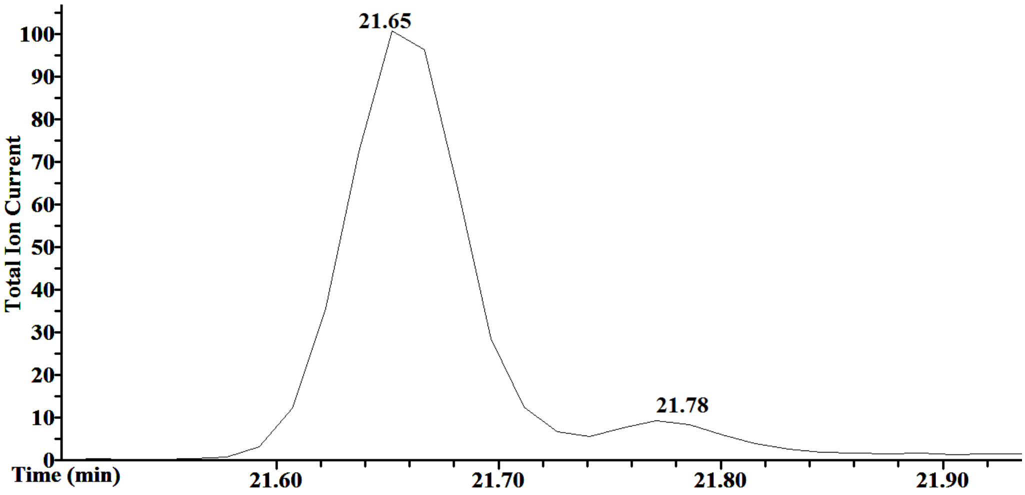

Catalyst = AuCu nanoparticles

References:

[1] P. H. Martinez, K. C. Hultzsch and F. Hampel, *Chem. Commun.*, 2006, 2221-2223.

Supporting Information

Characterization of nanoparticle catalysts:

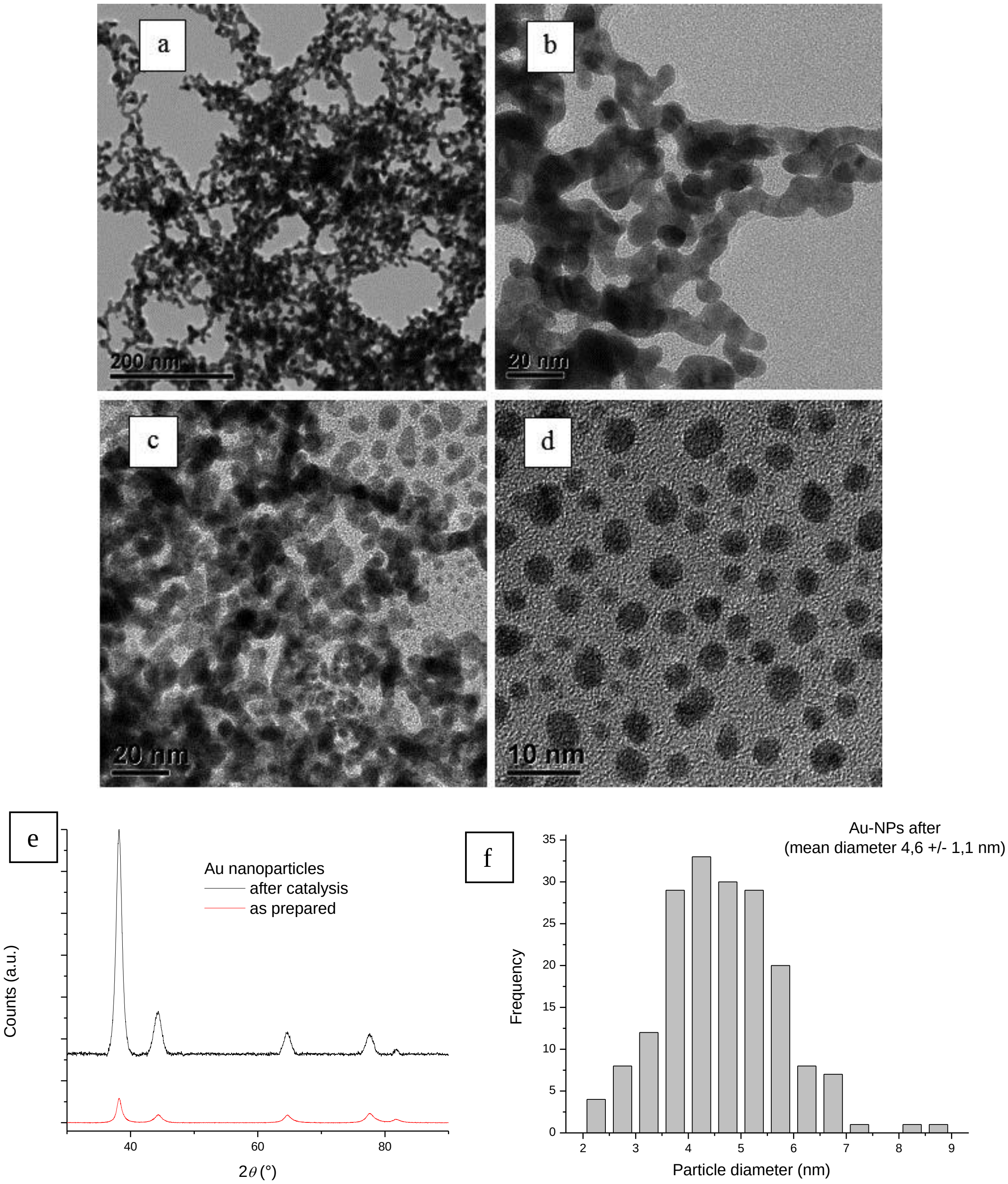

Figure S1. TEM images of monometallic Au nanoparticles as prepared (a, b) and after catalysis (c, d). XRD analysis of Au nanoparticles (e) and particle size distribution (f).

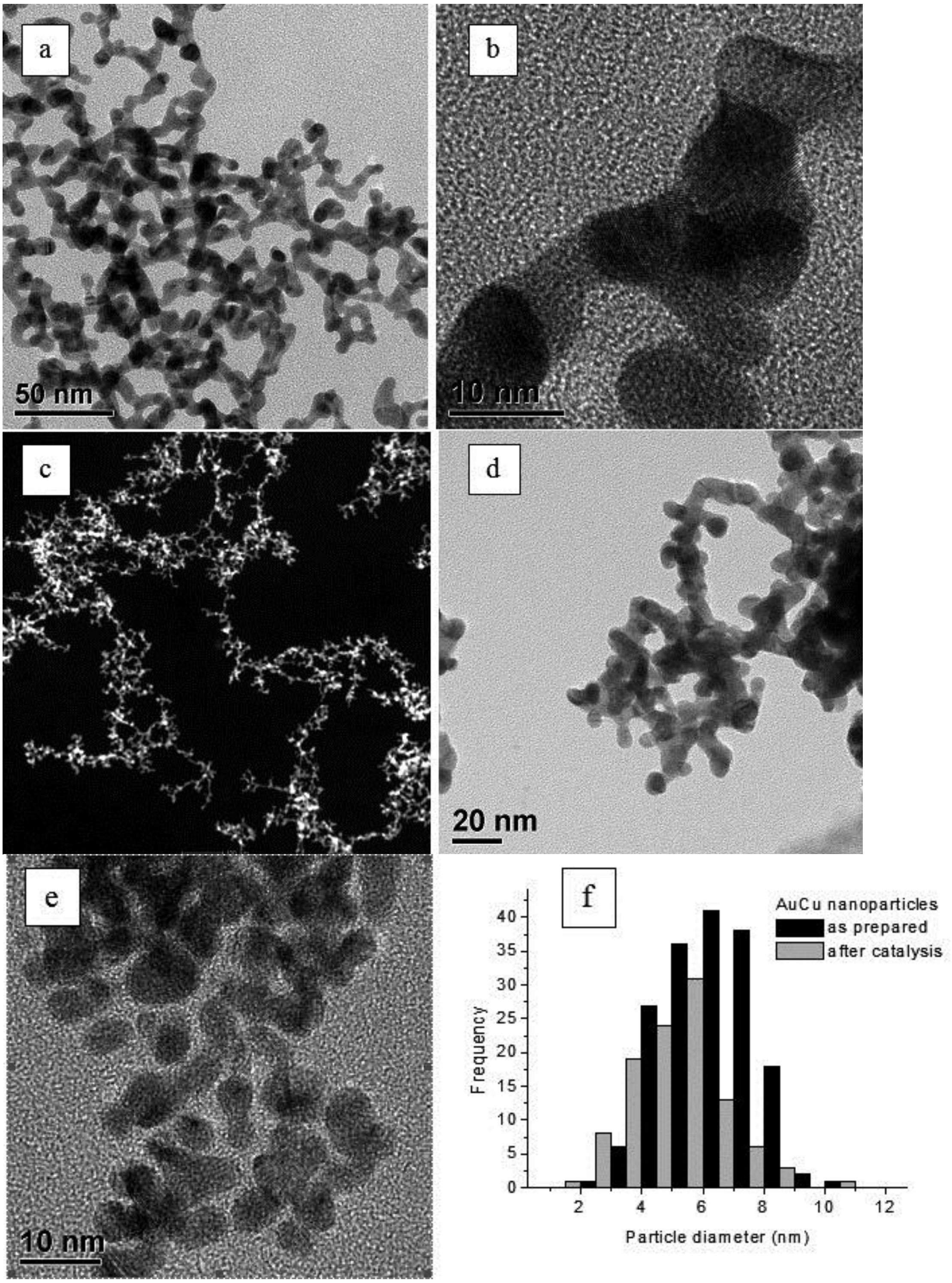

Figure S2. TEM and high angle annular dark field scanning transmission electron microscopy (HAADF-STEM) images of bimetallic AuCu nanoparticles as prepared (a, b, c) and after catalysis (d, e). Particle size distribution based on TEM analysis (f).

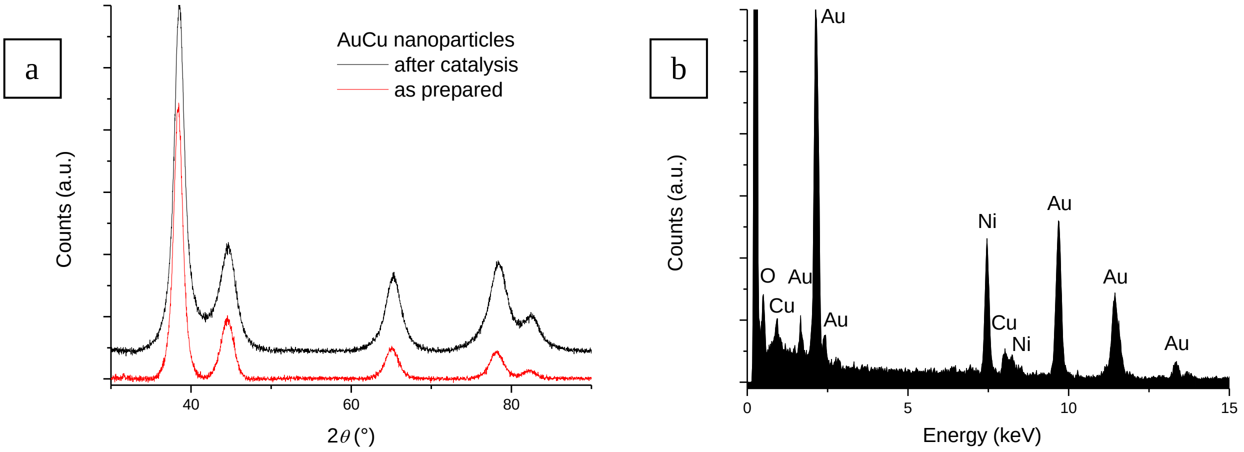

Figure S3. Powder XRD measurements (a) and EDX spectrum (as prepared, b) of the bimetallic AuCu nanoparticles.

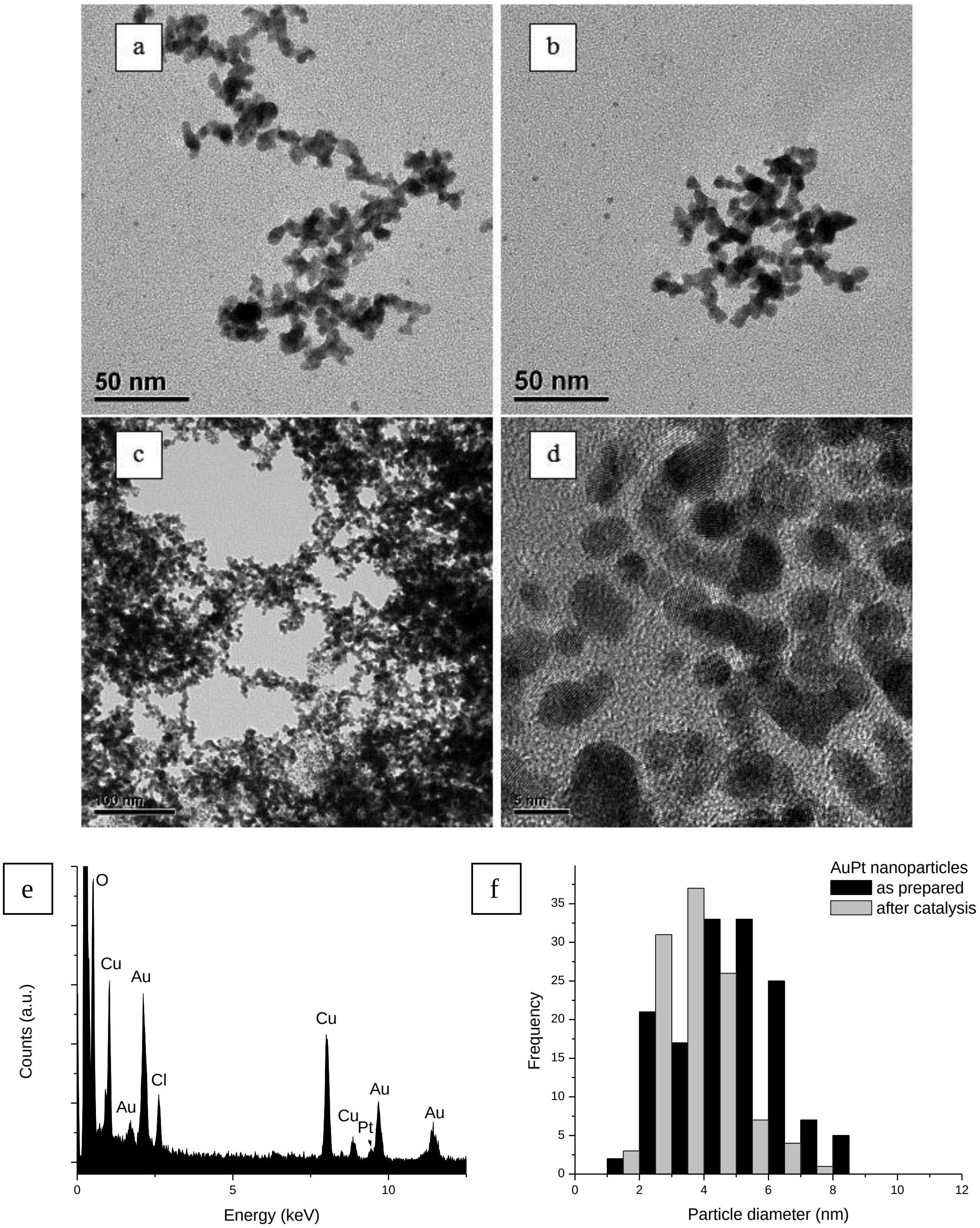

Figure S4. TEM images of bimetallic AuPt nanoparticles as prepared (a, b) and after catalysis (c, d). EDX spectrum as prepared (e) and particle size distribution of bimetallic AuPt nanoparticles (f).

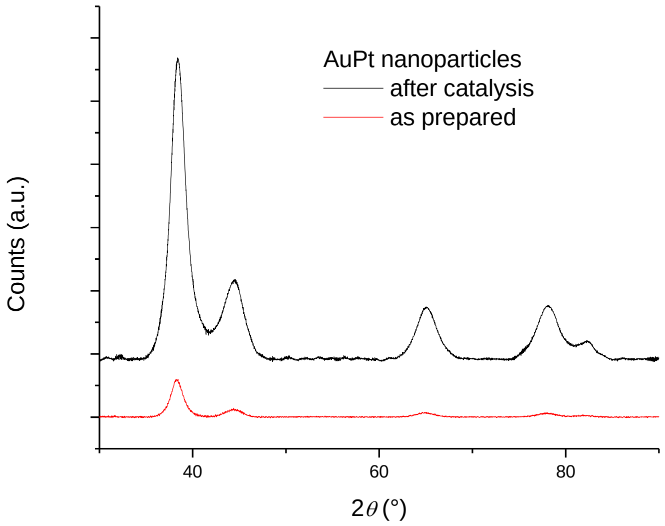

Figure S5. Powder XRD measurements of bimetallic AuPt nanoparticles.

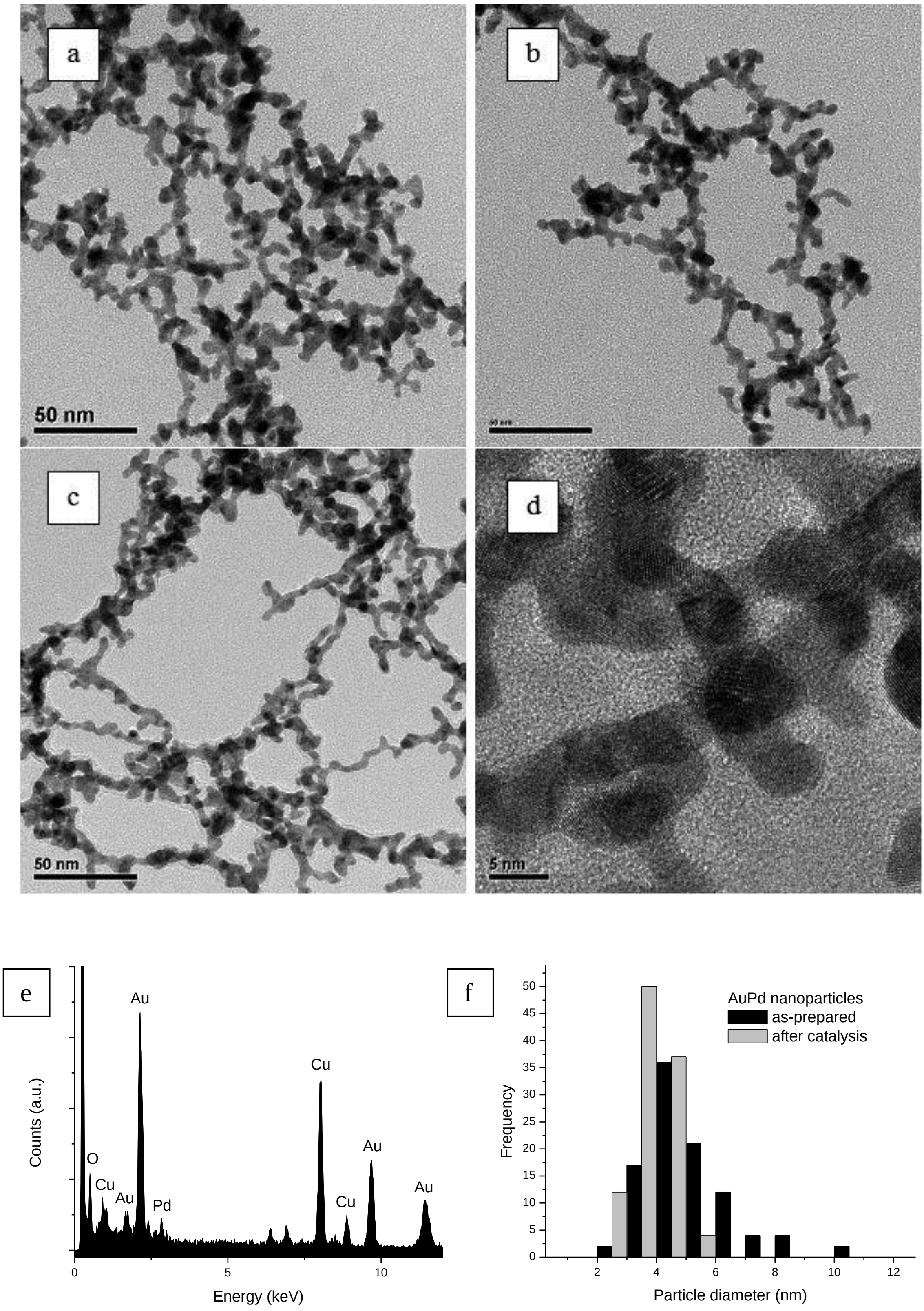

Figure S6. TEM images of bimetallic AuPd nanoparticles as prepared (a, b) and after catalysis (c, d). EDX spectrum of the particles (e) and particle size distribution based on TEM analysis (f).

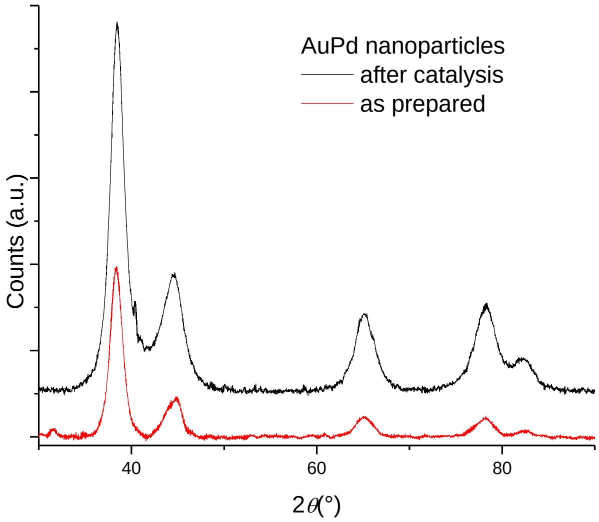

Figure S7. Powder XRD measurements of bimetallic AuPd nanoparticles.

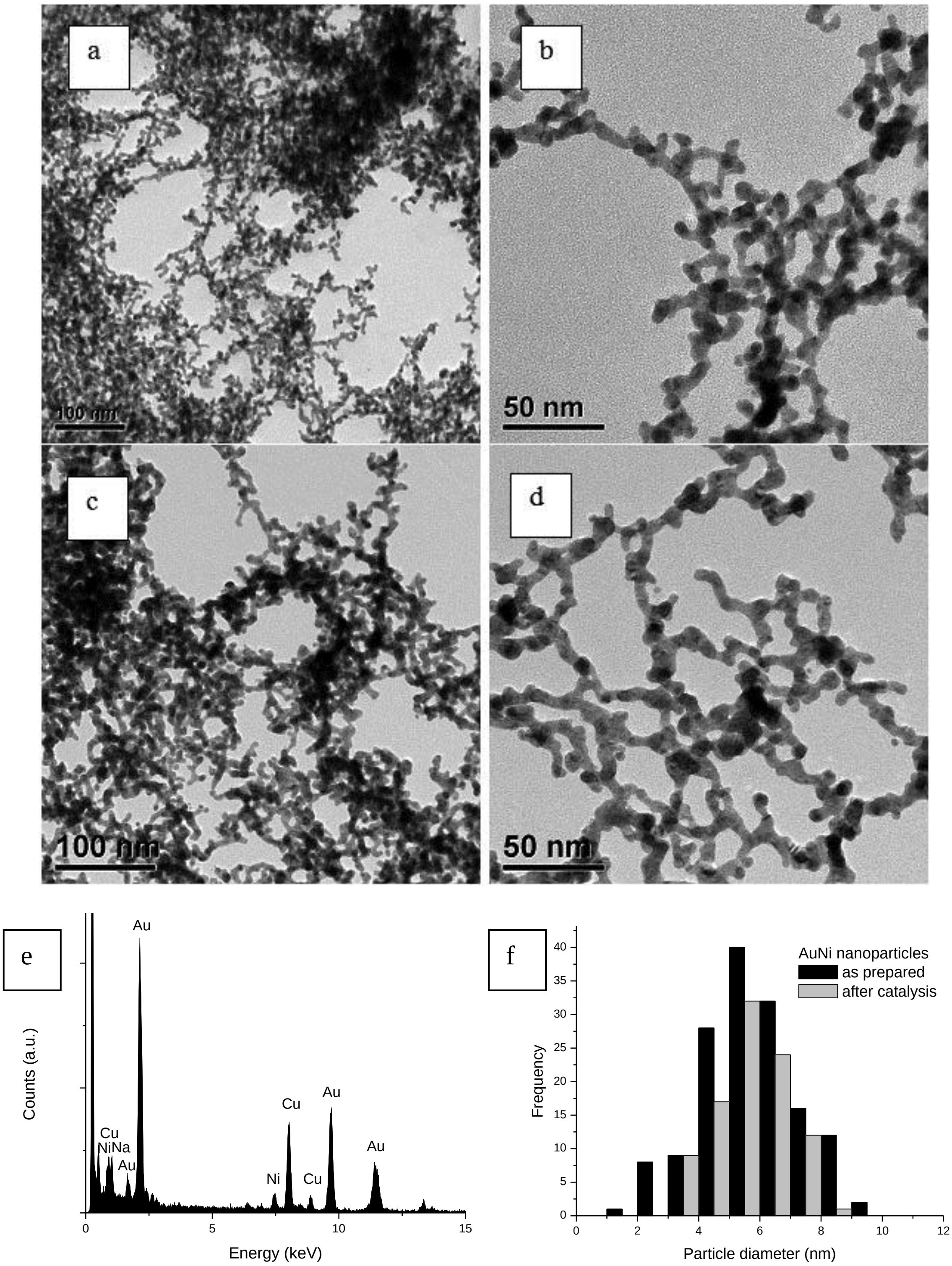

Figure S8. TEM images of the bimetallic AuNi nanoparticles as prepared (a, b) and after catalysis (c, d). EDX spectrum of AuNi particles (as prepared, e) and particle size distribution based on TEM analysis (f).

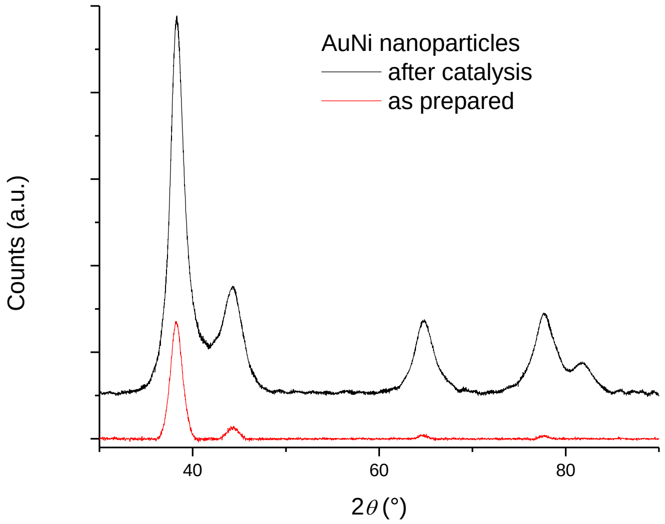

Figure S9. Powder XRD measurements of bimetallic AuNi nanoparticles.

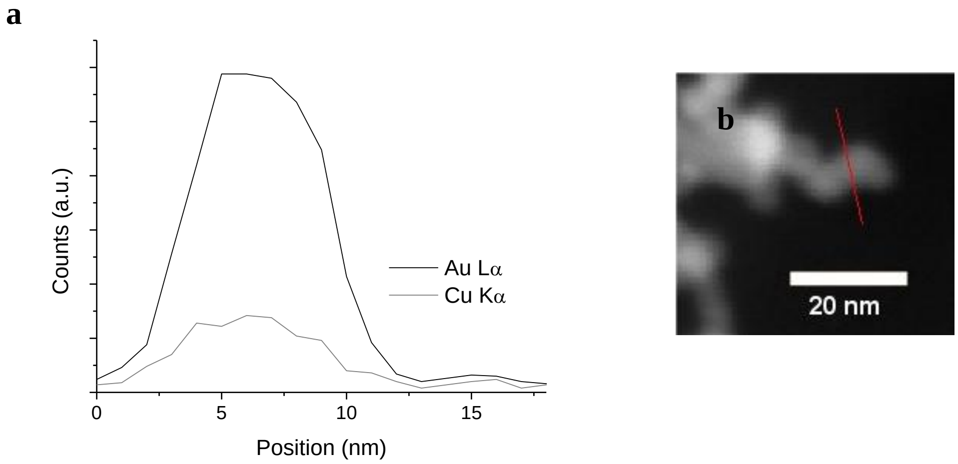

Figure S10. EDX line profile (a) and corresponding HAADF-STEM image (b) of a single bimetallic AuCu nanoparticle showing the alloy character of the particles.

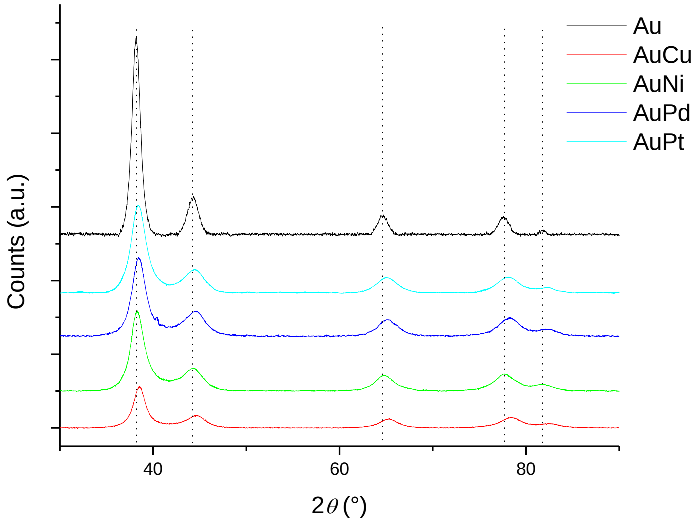

Figure S11. Comparison of the results of XRD analysis of monometallic Au and bimetallic AuPt, AuPd, AuCu and AuNi nanoparticles (after catalysis). The diffractograms show reflections of the cubic Au phase. A small shift is observed for reflections of bimetallic nanoparticles as compared to their monometallic counterparts due to the insertion of a second metal component.